RESPONSE OF AN ARTIFICIAL THORAX SYSTEM TO IMPACT

Harvey C. Shew and Werner Goldsmith
Department of Mechanical Engineering
University of California, Berkeley 94720, USA

ABSTRACT

Human thoracic models constructed of artificial materials were subjected to blunt impact by means of an automobile steering wheel striking the replicas at various velocities. Two systems, corresponding to conditions at mid-systole and end-diastole, respectively, were tested; these consisted of the rib cage, the vertebral column, two lungs, muscles, the diaphragm, a vascular network permitting blood flow and an added head form with neck musculature. The experimental results indicate that the bursting of the heart due to impact is more likely to occur during diastole than systole. Vessel strains were most significant in the aorta and the superior and inferior venae cavae.

INTRODUCTION

An estimated 35-40% of all traffic fatalities are either caused or complicated by thoracic injuries (1) that become life-threatening when breathing is seriously impaired as the result of broken ribs (flail chest) or a rib fragment pierces an organ or major vessel. Death can also result from blunt trauma by rupture of the heart or one of its major blood vessels (2), believed to be due to excessive hydrodynamic pressure and/or excessive strain (2-4). Common locations of vascular rupture were found at the insertion of the inferior vena cava into the right atrium, and on the aorta either just below the insertion of the ligamentum arteriosum or just above the aortic valve; the latter was explained as being due to to the lower strength of the aorta in this isthmus. Age appears to be an important factor in assessing injury tolerance due to the progressive weakening and reduction of extension of these tissues (5).

Previous work in thoracic trauma includes clinical or autopsy studies, analytical or mathematical modelling, use of live or dead animals in real or simulated accidents (3, 6), use of human volunteers in low-level, non-injurious tests (7) and employment of cadavers or ATD's in replicated accidents; the latter experience problems of reproducibility and biofidelity, respectively (7-9). Construction of suitable dummies has thus far concentrated on the system level and is capable of mass production at a reasonable cost. The present structure, on the other hand, was created on the basis of an optimal biofidelity of its individual components as well as of its global behavior which is feasible only for construction of a single or an extremely limited number of replicas. The system represents an improvement of an earlier model (10) which was also subjected to a different loading mode. Development and instrumentation of the current unit also utilized the techniques employed in the composition of a replica of a human head/neck/upper torso structure (11).

MODEL DEVELOPMENT

The objective of the construction of the model included the replication of the most important mechanical properties of the thoracic organs involved in injuries, i.e. the heart, its vasculature and the lungs, to install them in reali-

stic replicas of the human thorax, to subject the structure to steering-wheel impacts against the chest and to measure and record resultant pressures and deformations. Two units were constructed representing cardio-vascular conditions at mid-systole and end-diastole whose soft-tissue components, consisting of cloths, simulated the properties of their prototypes in two orthogonal directions. Use of two artificial heart valves and connection of the hearts to fluid systems simulating the input impedances of the aorta and pulmonary arteries and their installation in a more realistic thoracic model constituted a substantial improvement in replication over the earlier system (10). The cardiac muscle mass was also more closely represented by addition of sufficient quantities of water. Material selection was primarily based on the quasi-static data of (5) with the assumption that rate-dependence would not be a significant factor (12).

Simulation of the impedance of the major vessels, necessary to produce correct blood flow due to the impact, was accomplished by a parallel capacitor and flow resistor (13). Inversion of model and striker motion was designed to reduce spurious signals superposed on pressure and elongation records that resulted from vibrations of the transmission lines. Literature data and the hypothesis that the heart can be represented as a thin-walled spherical vessel produced the load-deformation curves shown in Fig. 1 for systolic and diastolic conditions. Their similarity prompted the use of the same material for the systolic and diastolic heart, with the wall of the former somewhat smaller and hence experiencing higher pressures at lower contained fluid volumes.

It was also assumed that (a) the heart cycle is sufficiently slow so that it could be modelled as a static, non-pumping system for the present loading, (b) the myocardium could be represented as a fiber-reinforced composite with properties intermediate between that of the fiber denoting that of the muscle

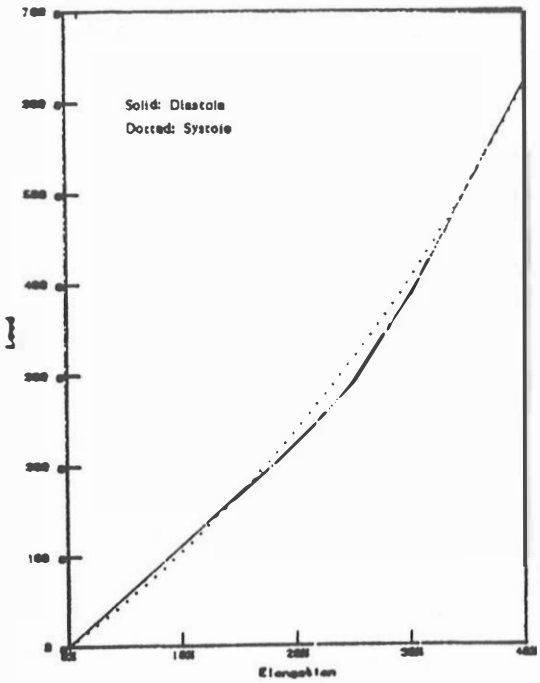

Fig. 1 Load-Deformation Curves of the Systolic and Diastolic Heart

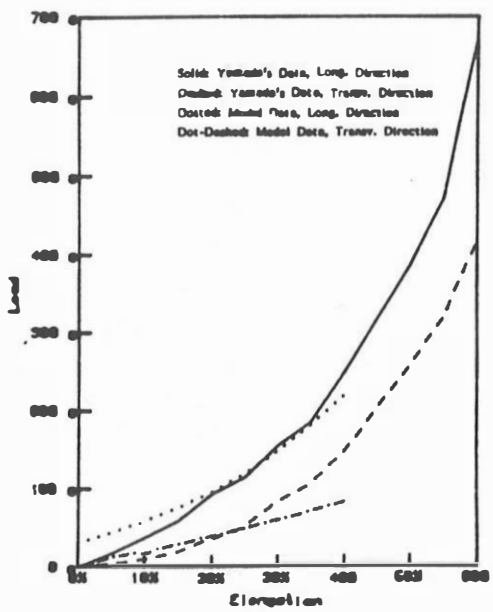

Fig. 2 Load-Elongation Curve of the Aorta

in the principal direction and that of the myocardium in the transverse direction, thus avoiding the actual cardiac fiber orientation, (c) the interstitial volumes of the thorax could be modelled as voids, (d) the dynamic response of the 60 lb system could be obtained from a model comprising the thorax, an added head form attached superiorly to T1 with supporting neck and back musculature and an added mass, (e) the pericardium could be neglected for the purpose of the present study, and (f) an additional 200 g of water added to that normally contained in the heart chambers would represent the actual total heart mass since the cloth chambers accounted for only a total of 50g mass.

The model thorax was built around a commercial polyester plastic skeleton of a 5 ft 2 in male with 5 mm strips of rubber-embedded fabric (11) representing the sternal cartilage. Replicated vertebral disks were cut from 9 mm thick sheets of silicone rubber with Dow-Corning RTV 732 adhesive applied to all facing surfaces. Failure of this cement in the systolic model limited tests on that system to a maximum impact speed of 1.2 m/s. Ligamentous material was attached to the anterior surfaces and spinous processes of the vertebral column and to the right and left vertebral arches to simulate the effect of the longitudinal ligaments, the ligamenta flava and the supraspinal ligaments. Satisfactory correlation of the system with cadaver data was obtained upon conduct of load-angular deflection tests. Upon attachment of ribs with ligamentous material, the deflection of the unit was again validated photographically upon application of weights. Silicone-embedded fabric simulating the intracostal muscles were attached with rubber adhesive. After installation of two lungs, sternal deflections from static loads of 20 and 50 lb were noted to fall within the range of values for a relaxed subject (2, 12).

The earlier technique for constructing the heart and blood vessels (10) was modified to accomodate blood flow and adjusted for the appropriate initial pressures. Load-strain properties of the myocardium were best simulated by a lycra-spandex leotard covered with a 0.001 in layer of iron-on decal material. Five layers of this composite were used for the left ventricles (LV) and the interventricular septa, two layers for the right ventricles (RV), and one layer each for the right and left atria (RA, LA). Fig. 2 portrays the comparison of the load-elongation characteristics for the aorta both in the longitudinal and the transverse direction for the model and prototype (5) under diastolic conditions, which have already been shown to be similar to that of systole.

Balloons of negligible stiffness were emplaced in the fabric chambers to render them impermeable. Prior to their insertion, pressure transmission tubes were installed in the balloons to measure chamber pressure. Artificial heart valves (Shiley, Inc.) were bonded inside the aortic and pulmonary valve rings of the diastolic model with rubber adhesive to allow for blood flow when opened by pressure differentials. Such a process was further simulated in the diastolic system by connecting the balloon liners for the atria and ventricles with 25.7 mm diameter silicon-primer treated latex rubber segments bonded to the liners. In the systolic heart, valve modelling permitted free blood flow from the ventricles into the aorta and pulmonary trunk by such bonding, but the atria were sealed to their corresponding ventricles to prevent communication, as opposed to the case for the diastolic model.

The great blood vessels were constructed of various leotards that displayed similar load-strain properties in the longitudinal and transverse directions relative to literature values (5) upon appropriate fiber alignment; additio-

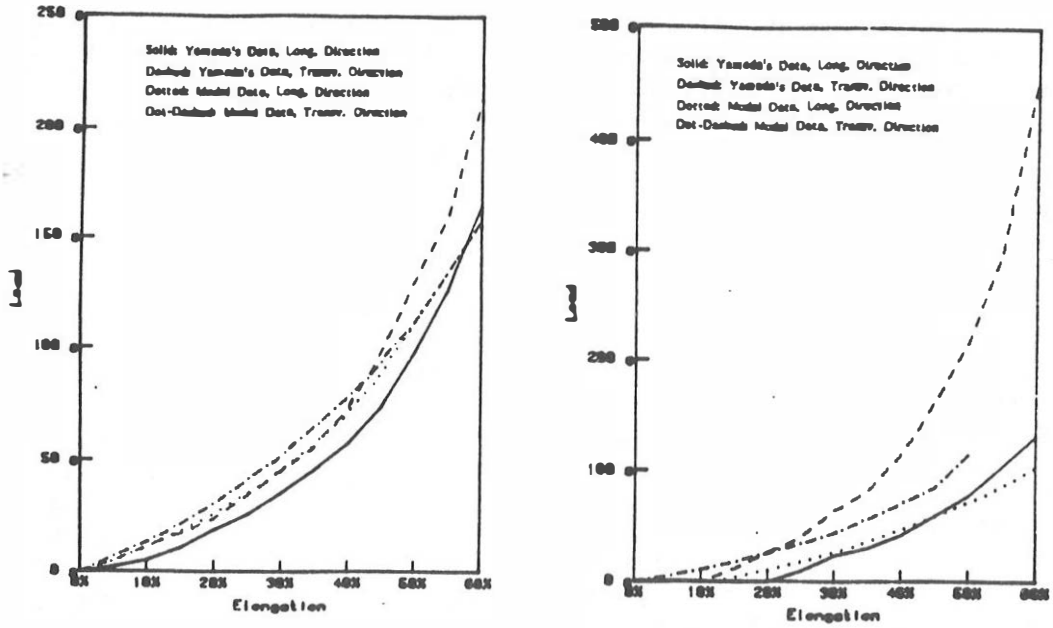

(a) (b)

Fig. 3 Load-Deformation Comparisons for (a) Pulmonary Artery (b) Pulmonary Vein

nal comparisons are portrayed in Fig. 3. Twelve vessels were constructed for each model: the aorta (AO); the brachiocephalic artery; the left common carotid and left subclavian arteries; the inferior and superior venae cavae; the right and left pulmonary arteries (PA) including their trunk, and the right and left superior and inferior pulmonary veins, all prestretched at least the equivalent of 17% physiological strain. The true prestrains of some vessels differed because they were most appropriately modeled by cloths with offset load-strain curves. Other construction details are presented in (12).

Lungs were cast from Dow-Corning 3-6548 RTV Silicon Foam in previously-developed molds, trimmed to fit the thoracic cavity of the skeletons and attached to the inner rib cage surface with rubber adhesive. Since the mechanical influence of the pericardium during impact is minimal, only its support function was modelled. The replica, a sheet of latex rubber gently wrapped around the heart and greater blood vessels, was bonded to the sternum with rubber cement. Literature values of skeletal muscle cross-sectional areas (14) were combined with stress-strain data (5) for muscle parallel to the direction of the muscle fibers to determine the load-strain curves for the intercostal muscles and the diaphragm.

INSTRUMENTATION AND DATA ANALYSIS

Six pressure transducers were used in this study, consisting of 20 ml syringes connected at one end to 0.030 in I.D. medical grade silastic tubing of 2 ft length and terminated at the opposite end by 0.2 mm thick steel diaphragms of 1.75 in diameter. Semi-conductor strain gages with a gage factor of 112 were cemented to the central diaphragm region to provide pressure measurement. Twelve commercial elongation gages consisting of mercury-filled distensible tubes were mounted on soft tissue replicas by rubber adhesive with at least

10% prestrain when the vessels were stretched to their correct physiological lengths and used to ascertain strain histories. A piezoresistive accelerometer (7264-200 Endevco) with a frequency range from 0 to 1000 Hz was attached to the striker, considered to be rigid, whose output multiplied by the mass of the striking cart provided the force history applied to the target. Eighteen signals were monitored with a DEC LSI-11/12 microcomputer by means of 2 analog-to-digital converters. The boards have a resolution of 12 bits in the differential mode and 10 bits in the pseudo-differential mode due to increased noise.

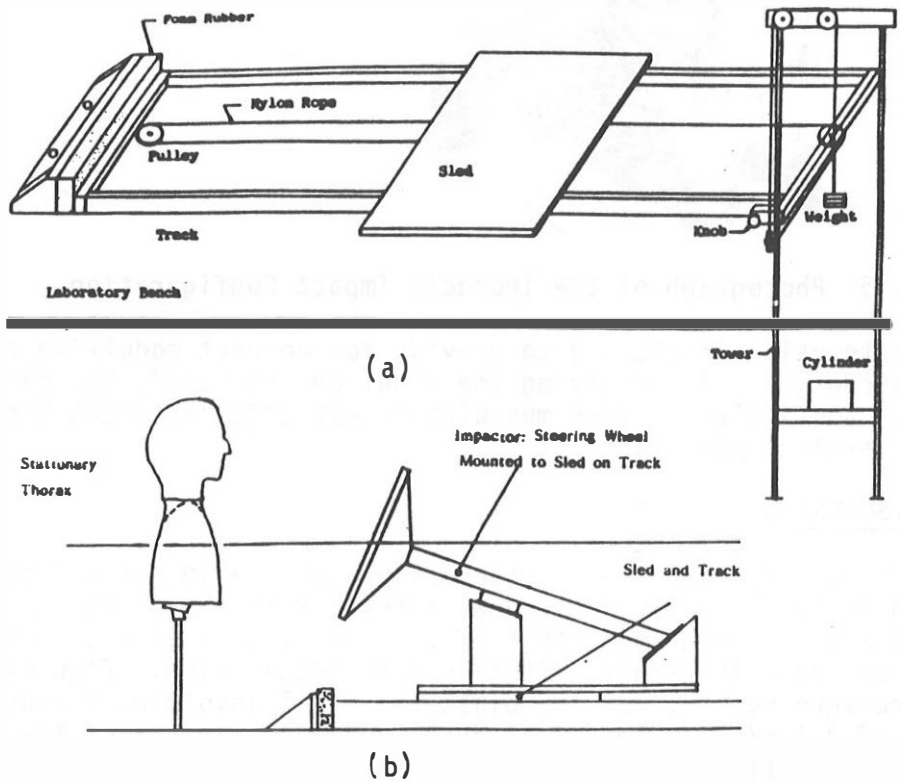

Fig. 4 Impact Configuration: (a) Sled Arrangement (b) Striking Conditions

The striker system, shown in Figs. 4 and 5, consisted of a steering column from a 1970 F10 Datsun station wagon supported by a 46 x 46 x 2 cm sled mounted on a 2.5 m long track (10). A rope passing over a pulley system accelerated the sled when weights attached to the other end were dropped from a 2.6 m tower; coasting of the sled occurred after the weight hit the ground until impact of the steering wheel with the thoracic model occurred. In view of the reversal of the motion relative to an actual accident, the mass of sled and steering column were adjusted to a value of 25.7 kg, the approximate mass of head and upper trunk of a 5ft 2 in tall male; this preserved the momentum of the collision. The model thoraxes were both mounted by fixing their T1 vertebrae to brass cups oriented at 20° to the horizontal. A 10.5 lb rubber-covered headform (Valjean, Detroit, MI) served to replicate the inertial effects of the head. It was bolted to a brass plate that was screwed to T1 and fabrics similar to those used previously (11) were superficially attached to headform and thorax in an attempt to replicate muscle effects. Thirty-five pounds of lead shot were then attached to the sides and rear of the thorax to bring its mass

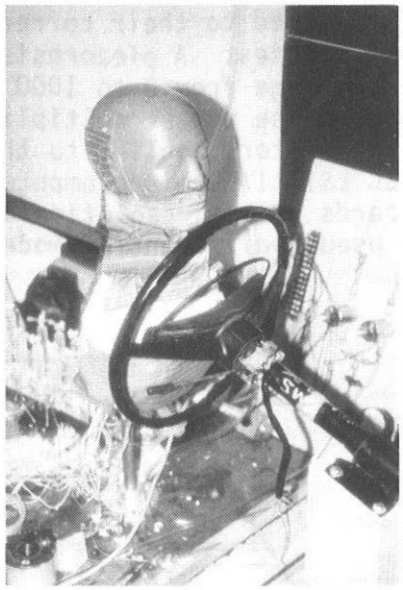

Fig. 5 Photograph of the Thoracic Impact Configuration

to an approximate value of 22.7 kg to provide for correct modelling of the inertia of the structure. After fixing the model on its stand, the heaform was bolted in place and its supporting musculature was adjusted until the head remained in the vertical position.

RESULTS AND DISCUSSION

Impact severity was increased by the successive application of weights of 3, 7, 10, 15, 20 and 50 lbs, but the structural integrity of the diastolic model was disrupted by the 50 lb weight and that of the systolic model was destroyed beyond the level of the 7 lb weight, limiting data acquisition. Figures 6 and 7 portray the pressure results for the diastolic model involving 3 runs at the maximum speed of 2.1 m/s (20 lb weight drop) and a comparison of the results at several speeds, respectively. Similar results for the systolic structure subjected to a speed of 1.2 m/s are presented in Fig. 8, and Fig. 9 compares the pressure response of the two structures at an impact velocity of 1.2 m/s.

Pressure increases in the heart, pulmonary artery and aorta begin at 50 - 100 ms after start of the record and peak around 400 ms for diastole and around 200 ms for systole. These rises are caused by the compression of the sternum into the heart. The subsequent drop in pressure is due to the rebound of the sternum to its normal position. For both models, the response of the left atrium was maximal, followed by the left ventricle for diastole and the aorta for systole. For diastole, this result was probably exaggerated because the model did not have functional atrioventricular valves and at least partly due to the difficulties in replicating the true shape of the heart which has a complex and asymmetric shape. In actuality, the rise in ventricular pressure due to impact would be expected to close the valves, avoiding the rise in atrial pressure. Since the model heart walls are much thinner than the prototype, they exhibit a much lower flexural rigidity. Hence the model ventricles were more spherical than realistic. This difference in shape is thought to have prevented the intimate contact of the ventricles with the sternum that would actually occur,

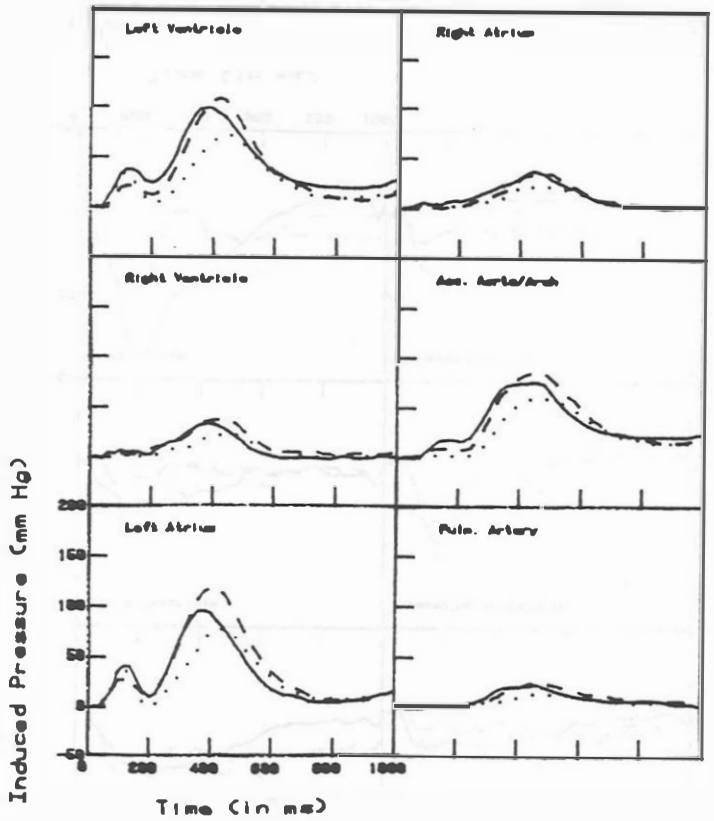

Fig. 6 Heart and Vascular Pressure Response for the Diastolic Model.
3 Runs at an Impact Speed of 2.1 m/s

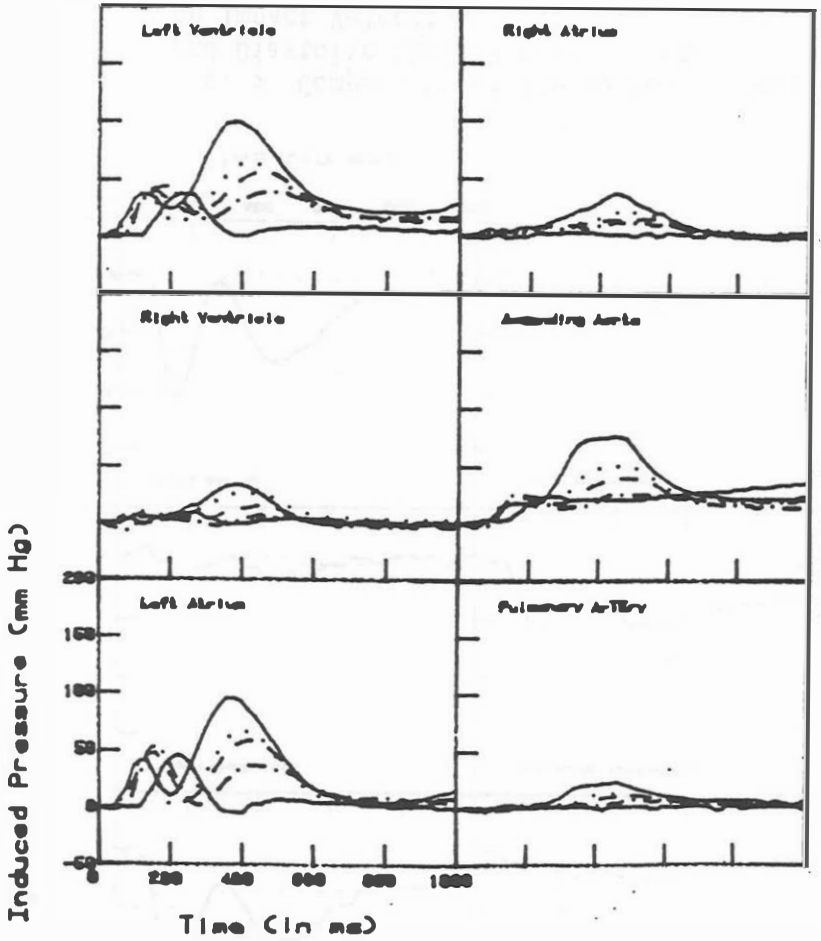

Fig. 7 Diastolic Pressure Response Comparison for Increasing Impact Velocity. Solid: 0.75 m/s; Dot-Dash: 1.3 m/s; Dash: 1.5 m/s; Dotted: 1.9 m/s; Solid: 2.1 m/s

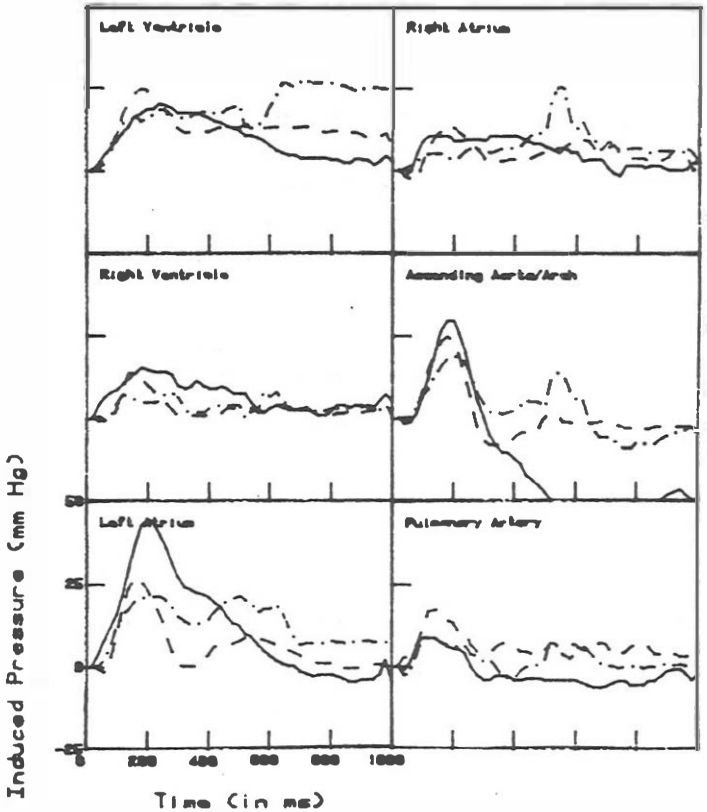

Fig. 8 Heart and Vascular Pressure Response for the Systolic Model.
3 Runs at an Impact Speed of 1.2 m/s

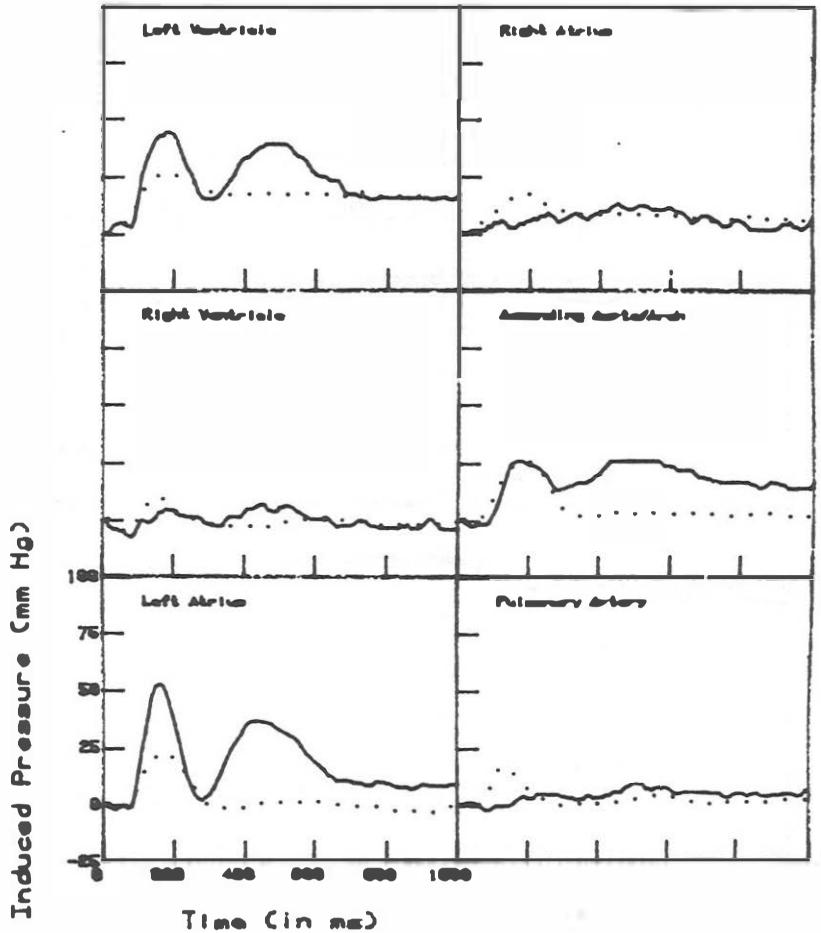

Fig. 9 Comparison of the Systolic (Dot) and Diastolic (Solid) Heart Pressures at an Impact Velocity of 1.2 m/s

resulting in somewhat lower pressure responses relative to the atria than expected.

Figure 7 exhibits a twin-peaked response of several components of the model, the first being of constant magnitude and the second growing with increasing impact levels. This can be explained in terms of the action of the functional aortic valve. After an initial pulse of sufficient magnitude to overcome the 65 mm Hg differential aortic pressure, the valve opens to relieve the system. The pressure rise in the aorta occurs at the time of these first pulse peaks. After the valve opens, the LV, the LA and the aorta responses are similar, except that the magnitude for the aorta is slightly diminished by fluid resistance and capacitance of the unit. This same twin-peaked behavior would also be expected for the right side of the heart, but could not be verified because another solenoid valve was not available to maintain the 15 mm Hg differential pressure between the RV and the pulmonary trunk.

Overall the diastolic pressure response was more repeatable and of greater magnitude than that of systole, as expected and shown in Fig. 9. The greater inertia of diastole compared to systole renders the heart less mobile in the former state. Thus, the systolic heart can more easily avoid being compressed by the displaced sternum than that for diastole, suggesting that low impact levels would tend to affect the heart more in its former state, as was observed. Also, the greater freedom of motion provided for this state of the heart due to its smaller size provides more mechanisms to dissipate the impact energy, explaining the greater variability in its responses to theoretically similar impact conditions. Finally, the added mobility of the heart in systole relative to diastole causes the former to reach its maximum compression, and thus its maximum pressure earlier than in the latter state, producing the earlier occurrence of the systolic peak pressure.

The strain response of the heart chambers, aorta and pulmonary artery is shown for three runs at an impact speed of 2.1 m/s involving the diastolic model in Fig. 10 and a comparison for the response of this system to various impact velocities is presented in Fig. 11. Similar information is provided in Fig. 12 at an impact speed of 1.2 m/s for the systole and Fig. 13 provides the response comparison at the same velocity for the diastolic and systolic models. Vascular diastolic model strains generated at various velocities are shown in Fig. 14, and a comparison of these strains for the two models at an impact speed of 1.2 m/s is presented in Fig. 15.

Cardiac strains are believed to be caused by local bending and elongations and are probably highly location-sensitive. Problems in the control of placement of the elongation gages resulted in some disparities of the strain results. These strains are due to motion caused by impact of body segments on either end of the particular blood vessel. For the model aortas, strains were due to heart motion and the extension of the entire thorax with respect to the fixed end of the descending aorta. Strains in the venae cavae were caused by heart displacement and, for the superior vena cava, extension of the head since it was attached to the bottom of the headform mounting plate, while, for its inferior counterpart, this occurred by extension of the entire thorax, since the inferior vessel was fixed similar to that of the descending aorta. Although flexion of head and thorax is actually seen in actual steering-wheel collisions, the present kinematic reversal produced an extensional response. Strains

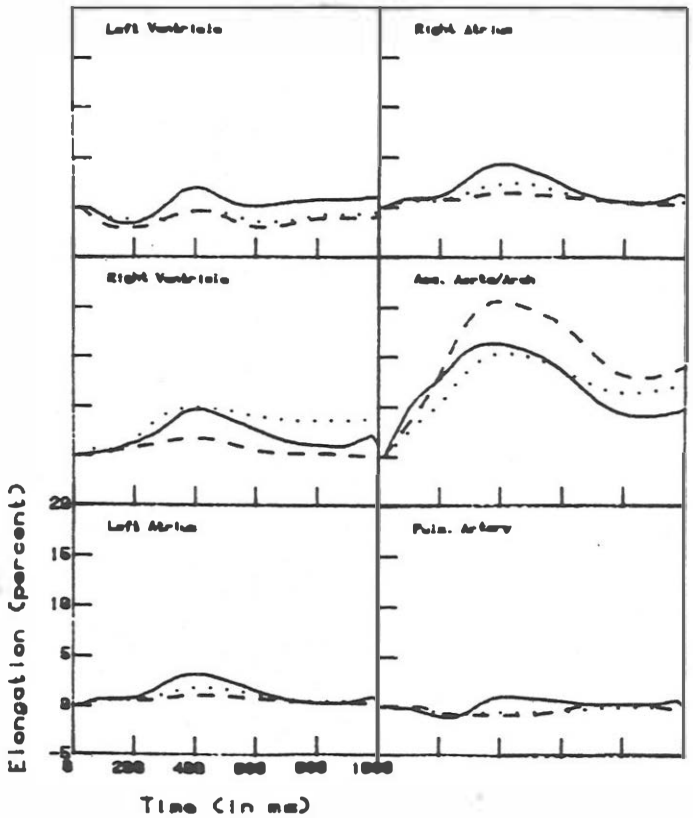

Fig. 10 Heart and Vascular Strain Response for the Diastolic Model
3 Runs at an Impact Speed of 2.1 m/s

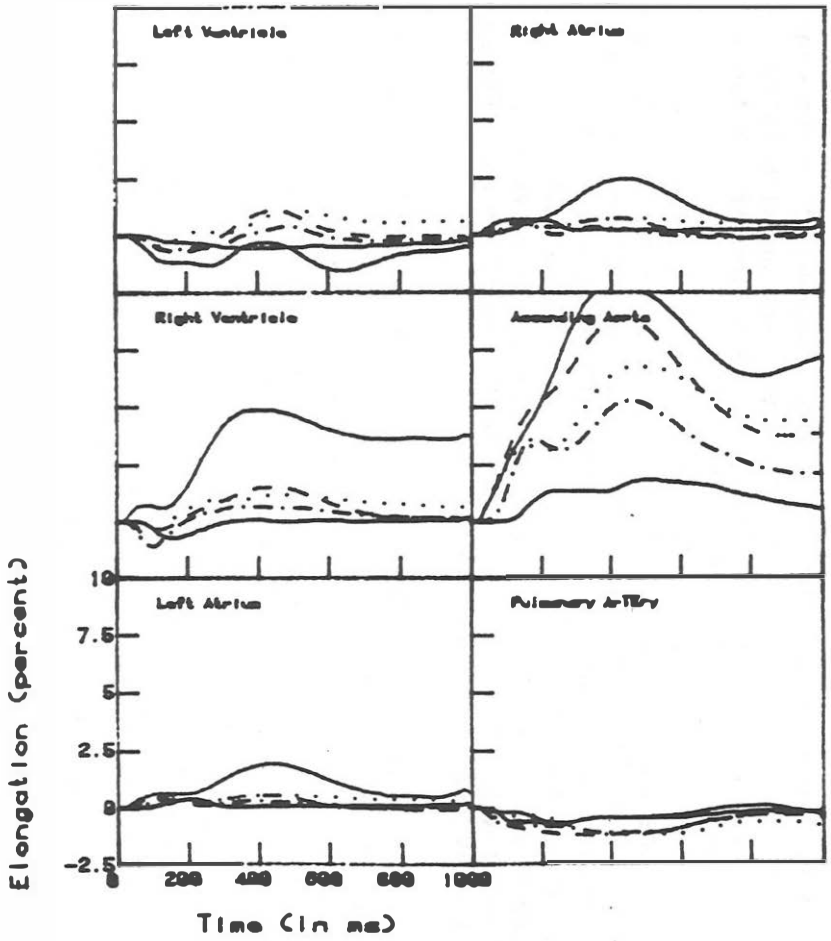

Fig. 11 Diastolic Vascular Strain Response Comparison for Increasing Impact Velocity. Solid: 0.75 m/s; Dot-Dash: 1.3 m/s; Dash: 1.5 m/s; Dotted: 1.9 m/s; Solid: 2.1 m/s

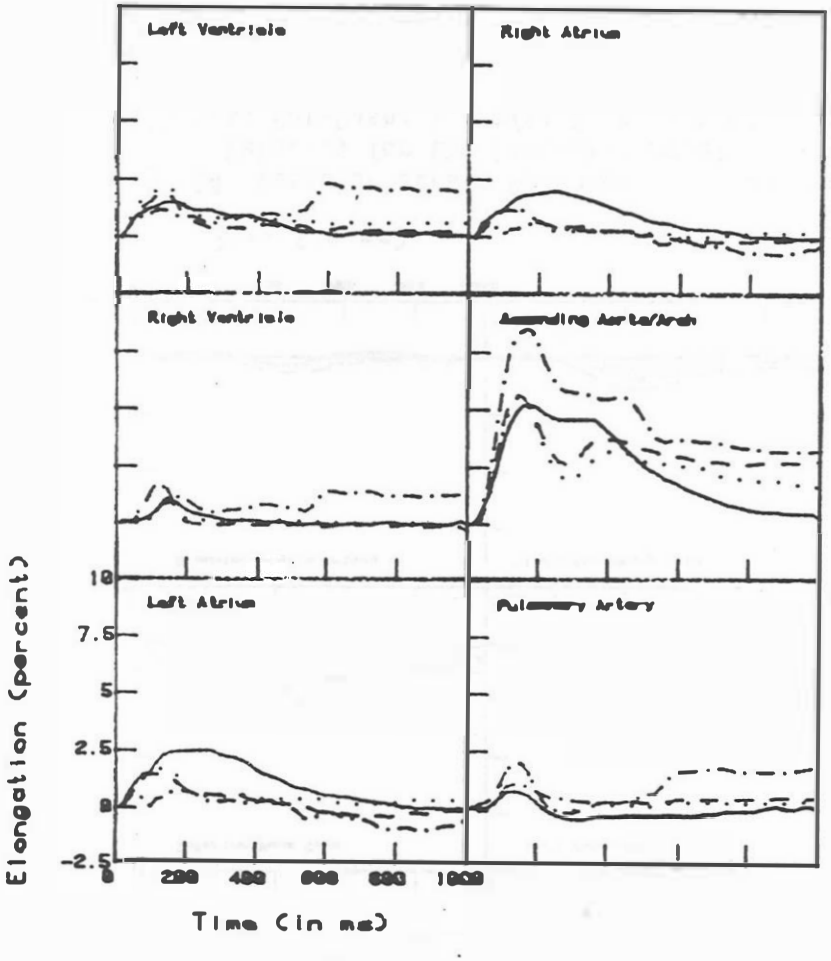

Fig. 12 Heart and Vascular Strain Response for the Systolic Model.
4 Runs at an Impact Velocity of 1.2 m/s

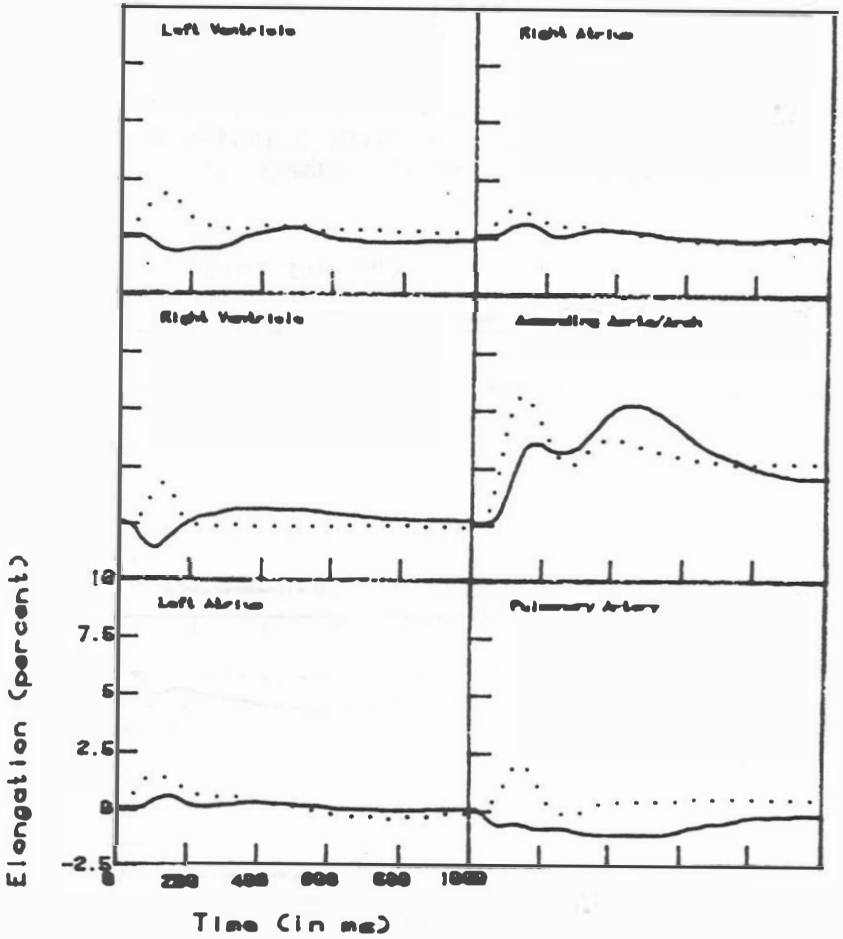

Fig. 13 Comparison of the Strain Response of Heart and Vessels for the Systolic (Dotted) and Diastolic (Solid) Models at an Impact Speed of 1.3 m/s

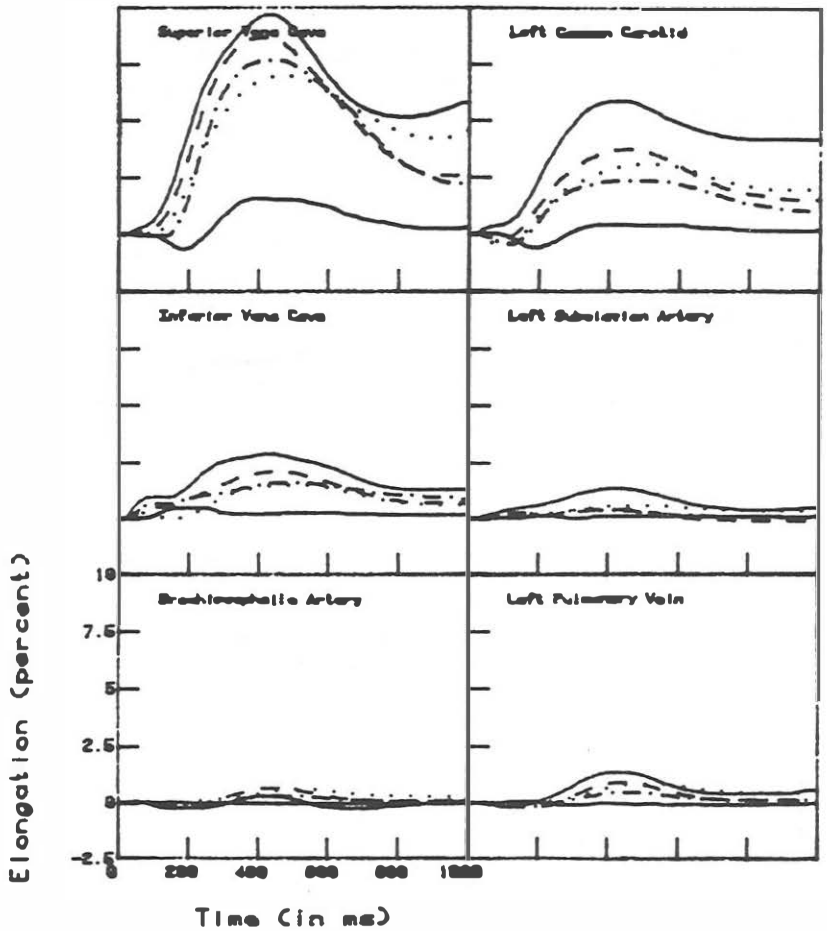

Fig. 14 Vascular Strain Response as a Function of Impact Velocity for the Diastolic Model. Solid: 0.75 m/s; Dot-Dash: 1.3 m/s; Dash: 1.5 m/s; Dotted: 1.9 m/s; Solid: 2.1 m/s

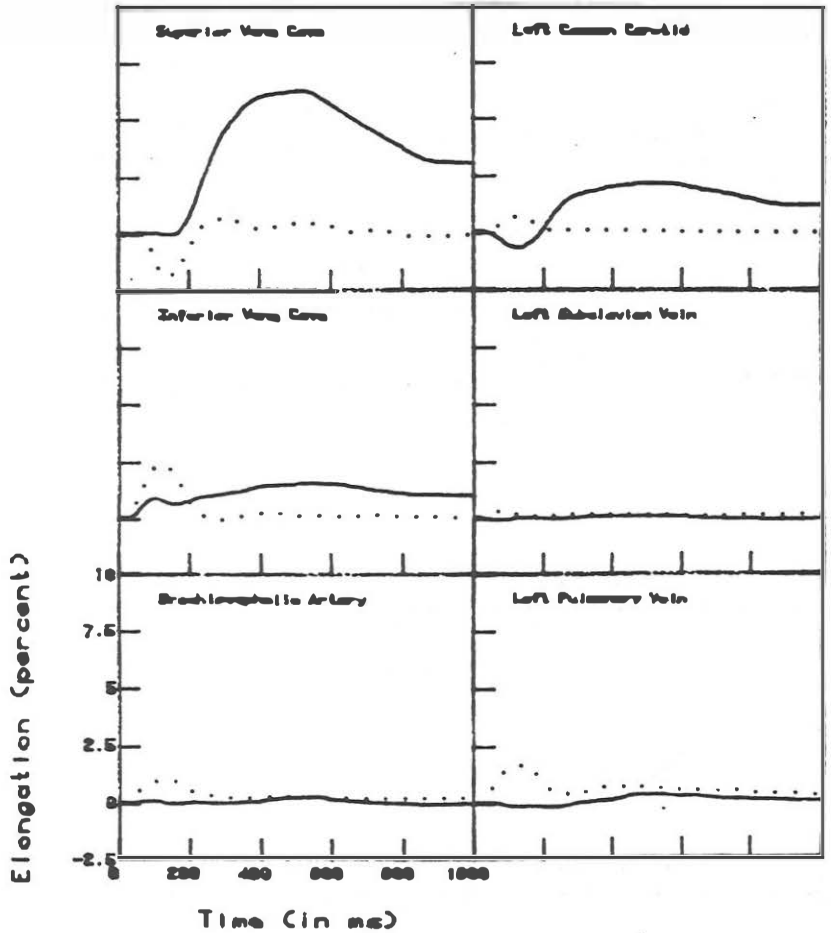

Fig. 15 Comparison of Vascular Strains of the Systolic (Dotted) and Diastolic (Solid) Model at an Impact Velocity of 1.2 m/s

in the pulmonary arteries and veins were caused by heart and/or lung motion. The brachiocephalic, left common and left subclavian arteries were stretched due to the displacement of the aortic arch from which these vessels originate.

Best repeatability of the strains also occurred at the lowest impact levels for both models, with the diastolic unit more repeatable than the systolic system. The largest strains observed in both models were in the aorta and the vena cavae, consistent with other experiments (2). The aorta exhibits a twin-peaked response at low impact levels, while at higher levels there is but a single peak. This discrepancy is probably related to the motion of the entire thorax. When the chest is hyperextended due to the collision, the aorta is stretched. The presence and absence of the twin-peaked behavior is presumed to be caused by the relative timing of heart and whole thorax motion. The most notable strain difference in the two models is the response of the venae cavae and left common carotid artery, Fig. 15. The superior vena cava was strained more than the inferior vessel in the diastolic model, while the converse was the case for the systolic system. These differences are attributed to a poor disk bond between vertebrae T11 and T12 that permitted the neck to hyperextend (as was also the case with bond failure at T1/T2). As the superior vena cava was attached to the plate on which the headform was mounted, this head motion was thought to stretch this vessel more than is realistic.

Acceleration histories consisted of a plethora of spikes so that not too much significance can be attached to the peak force values. Impact velocities ranged from 0.75 to 2.7 m/s for the diastolic units, corresponding to 34-450 J of energy, and 0.71 - 1.24 m/s for the systolic unit, representing 31-95 J of energy. The acceleration records were found to be reasonably repeatable.

A least square regression of the data for the 3 and 20 lb weights in the diastolic and for 3 and 7 lb weights for the systolic model was performed with peak pressures and strains as dependent and impact velocity and energy as the independent variable. Although poor, a better fit of the results was obtained by considering peak responses to be linear functions of impact energy. The best fit (lower subclavian artery strain) had a correlation coefficient of 0.856, while the worst was for the right atrium strain with a value of 0.720; the typical coefficient was 0.75. These data were then extrapolated to estimate impact energies at which fatal injuries would be sustained. Failure estimates for bursting pressures on the data of (15, 16) that reported a left ventricle bursting between 1¼ and 1-3/4 atm. The pressure failures were assumed to occur at 1.5 atm for the left ventricle, 3/4 atm for the right ventricle and 0.3 atm for the atria; no data were available for the aorta. Vessel strain failure was set at 70% (5); the results are shown in Table 1.

Although the data were acquired at impact levels much lower than the fatal injury threshold, their extrapolation provides at least estimates of fatal impact velocities that are consistent with the 15-20 mph fatal steering-wheel driver impact speeds suggested from previous cadaver testing (17). However, the impact durations found here are at substantial variance from those reported there, amounting to 60-100 ms and 30-40 ms for the two cases, respectively. This is attributed to (a) the lower dynamic stiffness of the models relative to cadavers, and (b) the difference in testing conditions. The most significant differences in response involved the impact pressure duration, about 200-600 ms in the present study and only 30-60 ms in (17). This variance is primarily due to the lower flexural rigidities of the artifical as

TABLE 1. Extrapolated Estimates of Impact Velocities at which Failure Occurs

DIASTOLE

Part	LV	RV	LA	RA	AO	Sup. VC	Inf. VC
Predicted Failure Speed, m/s	21	24	9	13	12	13	25

SYSTOLE

Part	LV	RV	LA	RA	AO	Sup. VC	Inf. VC
Predicted Failure Speed, m/s	21	25	11	12	9	23	14

compared to the real heart walls. Although the models exhibited very realistic load-strain properties, the stress-strain properties of the constituent cloths were about 3½ times as stiff as that of cardiac muscle. Hence the heart walls were made considerably thinner in order to replicate the chamber load-strain properties. However, the wall rigidities could not be accurately simulated at the same time with the materials available. For example, the model left ventricle walls were about 3.2 mm thick compared to the 11 mm of an actual LV wall, so that the real heart wall has approximately twelve times the flexural rigidity of the model hearts. Hence, the models would be expected to deform significantly more and for a longer duration than that of the actual heart, which appears to be the case. However, this modelling deficiency should not significantly affect the strain response of the aorta and venae cavae. Injury mechanisms for this type of loading are suggested in (18).

Overall, the strain and pressure responses to steering wheel impact on the thorax were significantly lower than those found in indirect impact loading to this region (10) where strains of 15 percent in the inferior vena cava and pressure rises of 120 mm Hg in the LV were observed resulting from impact energies of about 36 J. Although no direct comparison can be effected due to the difference in loading, much of the difference is due to (a) the far greater mass of the present thorax which provides for a much lower impact velocity at an equivalent impact energy, (b) the greater number of available energy dissipation mechanisms of the current model, and (c) the greater constraint of the system described here and corresponding increased damping resulting from the presence of model lungs. The greater complexity of the current model and correspondence of some of the responses observed here compared to the data from cadaver tests indicate that it more closely replicates an actual traumatic event of this nature.

CONCLUSIONS

The overall strain responses of the two models constructed and tested appear to be qualitatively and quantitatively consistent with the literature, while the pressure responses are only qualitatively analogous. Based on the results of the experiments, the following conclusions have been drawn:

(a) The pressure response of the diastolic heart is greater than that of systole, while the vascular strains appear to be comparable. The diastolic pres-

sure rises suggest that bursting is more likely in this state than in systole.

(b) As expected, the aortic strains were the largest. The inferior and superior venae cavae also displayed significant deformations in response to impact.

(c) Because the heart is smaller and more mobile in systole than in diastole, its pressure and strain responses are more variable than those of diastole.

(d) The incorporation of an artificial aortic valve in the diastolic model was found to affect the qualitative impact behavior of the system.

(e) The constitutive modelling approach employed in this study is promising. Many of the construction techniques used in this investigation could have application in the employment of artificial organs, most notably those in the cardiovascular system, to commercial anthropomorphic dummies.

(f) Flexural rigidities of the heart walls, as well as their load-strain properties, must be correctly simulated if accurate pressure responses to impact are to be obtained.

ACKNOWLEDGMENT

This paper was extracted from the M. S. Thesis of the first author, performed at the University of California, Berkeley. The authors are grateful for the sponsorship of the project by the National Institutes of Health under Grant No. AM 18384.

BIBLIOGRAPHY

1) Reddi, M. M., et al, "Thoracic Injury Mechanisms," Department of Transportation (U. S.) Technical Report No. DOT HS-801, August, 1975.

2) Collins, R., et al, "Thoracic Impact: Injury Mechanisms." In: Human Body Dynamics, ed. by D. H. Ghista. Oxford, Clarendon Press, 1982, pp. 38-126.

3) Roberts, V. L., Jackson, F. R., and Berkas, E. M., "Heart Motion due to Blunt Trauma of the Thorax," Proc. 10th Stapp Car Crash Conference, Paper No. 660800, 1966, pp. 146-150.

4) Mathern, R. Beitrag zur Zugfestigkeit der Aorta. Inaug. Dissertation, Heidelberg, 1972.

5) Yamada, H. Strength of Biological Materials, ed. by F. G. Evans. Baltimore, Williams and Wilkins Co., 1970.

6) Viano, D. C., et al, "Sensitivity of Porcine Thoracic Responses and Injuries to Various Frontal and a Lateral Impact Site," Proc. 22nd Stapp Car Crash Conference, Paper No. 780890, 1978, pp. 167-207.

7) Patrick, L. M., "Impact Force-Deflection of the Human Thorax," Proc. 25th Stapp Car Crash Conference, Paper No. 811014, 1981, pp. 471-496.

8) Patrick, L. M., and Levine, R. S., "Injury to Unembalmed Belted Cadavers in Simulated Collisions," Proc. 19th Stapp Car Crash Conference, Paper No. 751144, 1975, pp. 79-115.

9) Horsch, J. D., and Viano, D. C., "Influence of the Surrogate in Laboratory Evaluation of Energy-Absorbing Steering System," Proc. 28th Stapp Car Crash Conference, Paper No. 841660, 1984, pp. 261-273.

10) Shehadeh, G. N. Mechanical Response of an Artificial Heart System. Thesis (M. S.), University of California, Berkeley, 1983. Submitted for publication in the open literature.

11) Deng, Y.-C. Human Head/Neck/Upper Torso Model Response to Dynamic Loading. Dissertation (Ph. D.), University of California, Berkeley, 1985. Submitted for publication in the open literature.

12) Shew, H. C. The Response of an Artificial Thorax System to Impact Loads. Thesis (M. S.), University of California, Berkeley, 1985.

13) Westerhof, N. and Noordergraaf, A., "Reduced Models of the Systemic Arteries," Proc. 8th Int. Conf. Med. and Biol. Engineering and 22nd Conf. on Eng. in Med. and Biol., Chicago, July 20-25, 1969.

14) Weber, E. F., "Über die Langenverhältnisse der Fleischfasern der Muskeln im Allgemeinen," Berichte der Verhandlungen der Königlich-Sächsischen Gesellschaft der Wissenschaften zu Leipzig, Mathematische-Physische Klasse, August, 1851.

15) Kuno, Y., "The Significance of the Pericardium," J. Physiol., v. 50, p. 1, 1915.

16) Kuno, Y., "The Mechanical Effect of Fluid in the Pericardium on the Function of the Heart," J. Physiol., v. 51, p. 227, 1917.

17) Kroell, C. K., Schneider, D. C., and Nahum, A. M., "Impact Tolerance and Response of the Human Thorax II," Proc. 18th Stapp Car Crash Conference, Paper No. 741187, 1974, pp. 383-457.

18) Horsch, J. D., et al, "Mechanism of Abdominal Injury by Steering Wheel Loading," Proc. 29th Stapp Car Crash Conference, Paper No. 851724, 1985, pp. 69-78.